Volume 1 | Number 1 | Jan 2013 | Pages 1–100

PCCP

Physical Chemistry Chemical Physics
www.rsc.org/pccp

ROYAL SOCIETY
OF CHEMISTRY

ROYAL SOCIETY
OF **CHEMISTRY**

www.rsc.org/pccp

SO₂ – Yet Another Two-Faced Ligand

Jingbai Li, Andrey Yu. Rogachev[*]

Department of Biological and Chemical Sciences, Illinois Institute of Technology, Chicago,

Illinois 60616, USA

To whom correspondence should be addressed:

E-mail: andrey.rogachev@iit.edu and/or andrey.rogachev@gmail.com

Abstract

Experimentally known adducts of SO_2 with transition metal complexes have distinct geometries. In the present paper, we demonstrate by a bonding analysis that this is a direct consequence of sulfur dioxide acting as an acceptor in one set, square-planar complexes of d^8 and linear two-coordinated complexes of d^{10} transition metals, and as a donor with another compounds, well-known paddle-wheel $[Rh_2(O_2CCF_3)_4]$ and square-pyramidal $[M(CO)_5]$ (M=Cr, W) complexes. Bonding energy computations were augmented by the Natural Bond Orbital analysis (NBO) and Energy Decomposition Analysis (EDA). When the SO_2 molecule acts as an acceptor, bonding in the bent coordination mode to the axial position of d^8 or d^{10} metal center, the dominant contributor to the bonding is LAO(S) (Lewis Acidic Orbital, mainly composed of p_x-orbital of S atom) as an acceptor, while a d_z^2 orbital centered on the metal is the corresponding donor. In contrast, the distinct collinear (or linear) coordination of the SO_2 bound at the axial position of the $[Rh_2(O_2CCF_3)_4]$ and/or $[M(CO)_5]$ is associated with a dominant donation from a lone pair localized on the sulfur atom, the $\sigma^*(Rh-Rh)$ and/or empty LAO(M) (mainly composed of d_z^2 orbital of the metal), respectively, acting as an acceptor orbital. The donor/acceptor capabilities of the SO_2 molecule were also checked in adducts with organic Lewis acids (BH_3, $B(CF_3)_3$) and Lewis bases (NH_3, $N(CH_3)_3$, N-heterocyclic carbene).

INTRODUCTION

The initial Lewis bond description of Werner coordination compounds was based on the assumption that the ligand is an electron pair donor to the Lewis acidic metal cation.[1] As coordination chemistry was developed it has become increasingly evident that the metal-ligand bond types cover the whole range of possibilities for the ligand behavior, starting from being a pure donor to an unambiguous acceptor. Unusual character of the bonding between a metal center and a ligand was first recognized by Pauling for CO and NO+.[2] He has found that these molecules are ambiphilic due to synergic bonding interactions, which occur in their complexes with transition metals. However, if these interactions occur simultaneously, the shape of the adducts remains almost unchanged by relative contributions of forward and back components, albeit such geometrical parameters as M–C and M–O bond lengths are quite sensitive to the weights of individual components of the bonding.

After Pauling's findings, ambivalent behavior was observed for other organic and inorganic molecules that have been used as ligands in transition metal complexes.[3] Recently, great interest has been shown in the coordination of Lewis acid ligands such as $AlCl_3$, BR_3 and SnX_4 to compounds of the late transition metals in their low oxidation state.[4] These molecules are often called Z-type ligands. Possible bonding in such systems as well as different synthetic routes was discussed in recent publications of Hill[5] and Braunschweig.[6] The majority of these ligands acts as pure Lewis acids and does not show characteristic geometrical changes.

In this paper we theoretically explore the coordination chemistry of SO_2, a small molecule that belongs to another important group of ambiphilic Lewis acids/bases with

pronounced geometrical signatures. Molecules of this type may function as either electron donors or acceptors *through the same atom*, but adopt different shapes depending on whether they act as Lewis acids or Lewis bases. This group of interesting ligands is exemplified by such well-known molecules as the already mentioned SO_2 and NO^+, and also by heavy dihalogens like I_2. Recently, a detailed theoretical analysis of the alternative bonding of I_2 was published[7] and this simple molecule was described as Janus-faced ligand with well-delineated geometrical signatures.

The story of SO_2 as a ligand in transition metal complexes started back in 1938, when the first adduct was reported.[8] In the 1960s it was first suggested that the geometries of SO_2 and NO^+ adducts of compounds like $[IrCl(CO)\cdot(PPh_3)_2]$ could be rationalized if these ligands are considered as electron acceptors, which interact with electron lone pair of the metal center in low oxidation state. Then, the Hückel molecular orbital theory was used to study SO_2 adducts.[9] It was qualitatively shown that due to the different topology (or "geometrical signature"[10]) of interacting frontier molecular orbitals of sulfur dioxide, the bonding model can be divided into three types, namely, σ^*, η^1, and η^2. When SO_2 acts as an electron donor, the interaction can be described as electron donation from the highest occupied molecular orbital (HOMO) of SO_2 to the available unoccupied orbital of the metal center (η^1 type) resulting to the linear geometry of the final complex (Scheme 1a). In the case of sulfur dioxide molecule playing the role of an acceptor, the interaction involves the lowest unoccupied MO (LUMO) of the SO_2 that accepts electron(s) from the transition metal lone pair (σ^*-type). This type of bonding is expected to lead to the bent geometry of the adduct (Scheme 1b). Importantly, these two types of interaction are mostly related to the reactivity of the sulfur atom in SO_2. The η^2 type involves both S and O atoms interacting

with metal center and is beyond the scope of this consideration. It is interesting to note here that a recent investigation of the I_2 molecule and its adducts with transition metal complexes revealed an opposite trend, in which the bent geometry corresponds to the donor behavior, whereas the linear shape agrees with an acceptor role of the dihalogen.[7]

Scheme 1
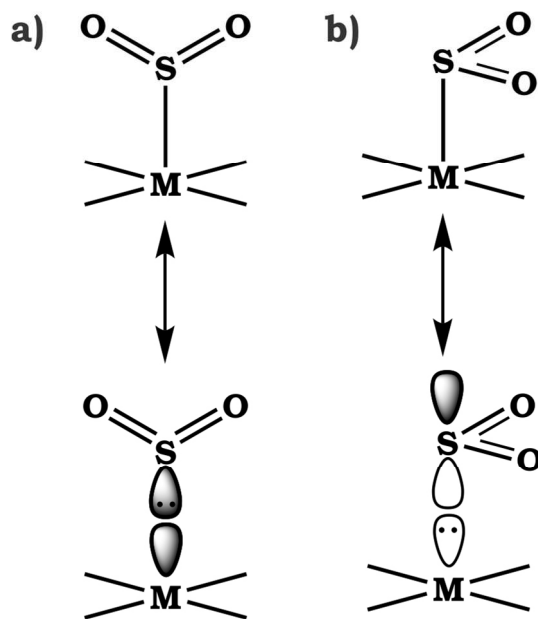
Since these pioneering investigations, the experimental coordination chemistry of the SO_2 molecule as a Lewis acid was substantially developed due to efforts of the group of van Koten.[11] Recent achievements in the field were previously reviewed.[10, 12] The interaction between SO_2 and transition metals was also studied with the help of density functional methods (DFT) aiming at stability of possible adducts.[13]

In this article, we present a comprehensive theoretical investigation of a series of transition metal complexes of SO_2. With the help of a combination of modern analytical tools of quantum chemistry, such as the natural bond orbital (NBO[14]) technique and energy

decomposition analysis (EDA[15]), the various bonding contributions in these intriguing organometallic systems are quantified. The questions we intend to shed light on are: Can SO_2 behave as a pure acceptor/donor in corresponding adducts? Or is its donor/acceptor behavior just obscured? In the process, we learned the features that make a ligand a potential acceptor, rather than, or in addition to, being a good donor. As model organometallic fragments for interaction with SO_2, two complexes, namely, platinum (II) square-planar [L(CH₃)Pt] (widely used by the group of van Koten[11]) along with its isoelectronic iridium (I) analogue [L'(CH₃)Ir], and rhodium (II) paddle-wheel [Rh₂(O₂CCF₃)₄] compounds were chosen (Scheme 2). These complexes were successfully used in the previous study of different behavior of I₂.[7] These models are ones where the axial ligand can show only one type of coordination behavior, donor or acceptor. The set was augmented by the linear complexes of d^{10} Pd(0) and Pt(0) with two trimethylphosphine ligands, for which adducts with SO_2 are known experimentally (albeit with much bulkier substituents at phosphorus atoms)[16] and classic Lewis acceptor [M(CO)₅] (M = Cr, W). The use of d^6 M(CO)₅ fragments, Lewis acids, to bound lone pairs is common – for a selection, see recent work.[17]

Scheme 2

X=C for M=Pt(II)
X=N for M=Ir(I)

M=Pt(0), Pd(0)

M=Cr, W
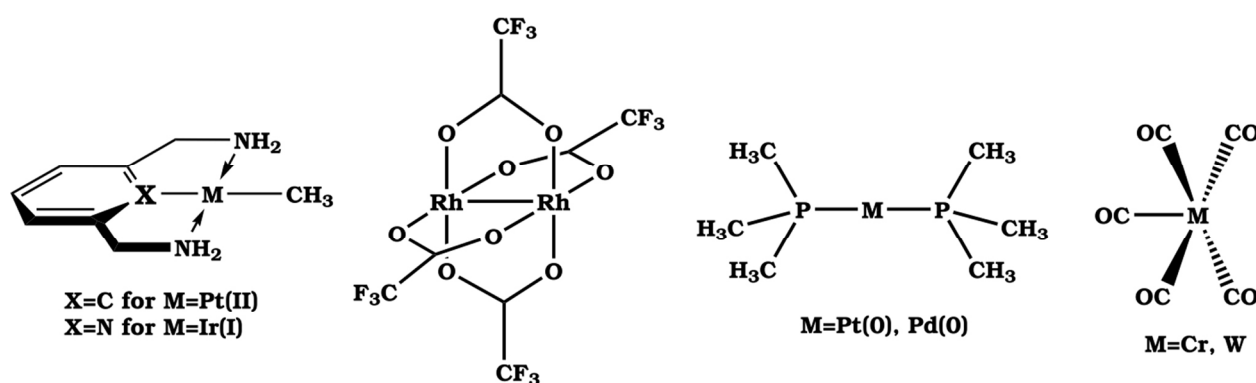
The potential acceptor/donor behavior of SO_2 was also investigated in adducts with pure σ-donors/acceptors such as amines and N-heterocyclic carbene (NHC)/BH_3 and $B(CF_3)_3$.

RESULTS AND DISCUSSION

Before we proceed with consideration of the bonding situation in adducts of SO_2 with transition metal complexes, it is instructive to qualitatively sketch the electronic structure of prototypic parent fragments. The electronic structure of all the organometallic fragments (except for linear $[(P(CH_3)_3)_2M]$, where M=Pt(0), Pd(0)) in terms of canonical MOs as well as their relationship with corresponding NBOs was previously considered in detail.[7,18] The electronic structure of the parent linear complexes of d^{10} metals will be considered as part of the general study of corresponding adducts with sulfur dioxide. Thus, we proceed to consider here only the SO_2 molecule.

Canonical MOs and NBOs of SO_2. Canonical MOs of SO_2 (Fig. 1 *right*) are quite familiar.[19] Leaving behind low-lying MOs, let's consider only frontier orbitals that are mainly responsible for the chemical reactivity of the molecule. These orbitals are actually the part of a manifold of p-type orbitals involving S and O atoms. Due to the mismatch in electronegativity of O and S, these orbitals are slightly more localized on the sulfur atom. From Fig. 1 (*right*) one can see that the LUMO is mostly localized on the sulfur atom and mainly formed by its p_x-orbital with some participation of p_x-orbitals of oxygen atoms in anti-bonding way (see 3D map in Fig. 2 *right*). This orbital is perpendicular to the plane of the SO_2 molecule. Thus, if one considers this MO participating in donor-acceptor interaction with an available electron lone pair (assuming SO_2 playing the role of an acceptor), the shape of the final adduct is expected to be bent.

The HOMO of SO_2 is quite delocalized and shows significant participation of all three atoms. Because of the symmetry, this orbital (a_1 for C_{2v}-symmetrical molecule) has a notable contribution from the s-orbital of the sulfur atom (see the right parts of Fig. 1 and Fig. 2). Considering the SO_2 molecule as a potential donor ligand in complexes with transition metal center, the shape of such adducts is expected to be linear (with the angle between M–S bond and plane of sulfur dioxide close to 180°).

The natural bond orbital technique gives a picture of the essential orbitals of SO_2 and the way these orbitals interact with metal fragment that is both similar and, in essential ways different from the canonical MO picture described above. As it was found previously,[7,18] the NBOs are well-localized for the case, where delocalization is not essential (lone pairs, when there are more than one in the molecule). In the case, where delocalization is essential (σ- and π-bonds), the corresponding natural bond orbitals are delocalized. This is what we see in Fig. 2 (*left*). In order to provide a better understanding of the relationship between localized NBOs and delocalized canonical MOs, the full diagram combining both types of orbitals was created (Fig. 1). This diagram clearly shows the direct relation between NBOs and MOs for the same system (starting from atomic orbitals of O and S atoms). For comparison, 3D maps of both NBOs and canonical MOs are presented in Fig. 2.

Since in most cases NBOs often enhance localization in a chemically intuitive way, we now proceed with considering changes of important MOs in the SO_2 molecule. Instead of four delocalized MOs originated from p-atomic orbitals (p_y and p_z sets), there are two sets of well-shaped σ- and σ*-NBOs (σ_A, σ_B and σ_A^*, σ_B^* in Fig. 2). The delocalized π-system of the molecule (occupied 1π, 2n and unoccupied 2π*) is now presented by the combination of

π-bonding S–O NBO, a corresponding anti-bonding (π^*) partner, and a p_x-lone pair located on another oxygen atom. The difference in electronegativity between S and O makes the π^*-NBO mostly localized on the sulfur. This orbital represents now what was previously called the LUMO in terms of canonical MOs and is responsible for the acceptor properties of the system. Note that such localization creates asymmetry in the electronic structure of SO_2. However, there is a paired resonance structure (of the equal weight) in which that asymmetrization is reversed, thus reconstructing the total symmetry of the system.

The lone pair centered on the sulfur atom in terms of NBO is a hybrid orbital (hereafter called s(S)) with substantial s-character (70% of s- and 30% of p-character).

Next, we will show that these two NBOs (occupied s(S) and empty π^*) are crucial for the adequate description of the donor-acceptor behavior of the SO_2 molecule in reactions with appropriate metal fragment(s). With consequent well-pronounced geometrical signatures.
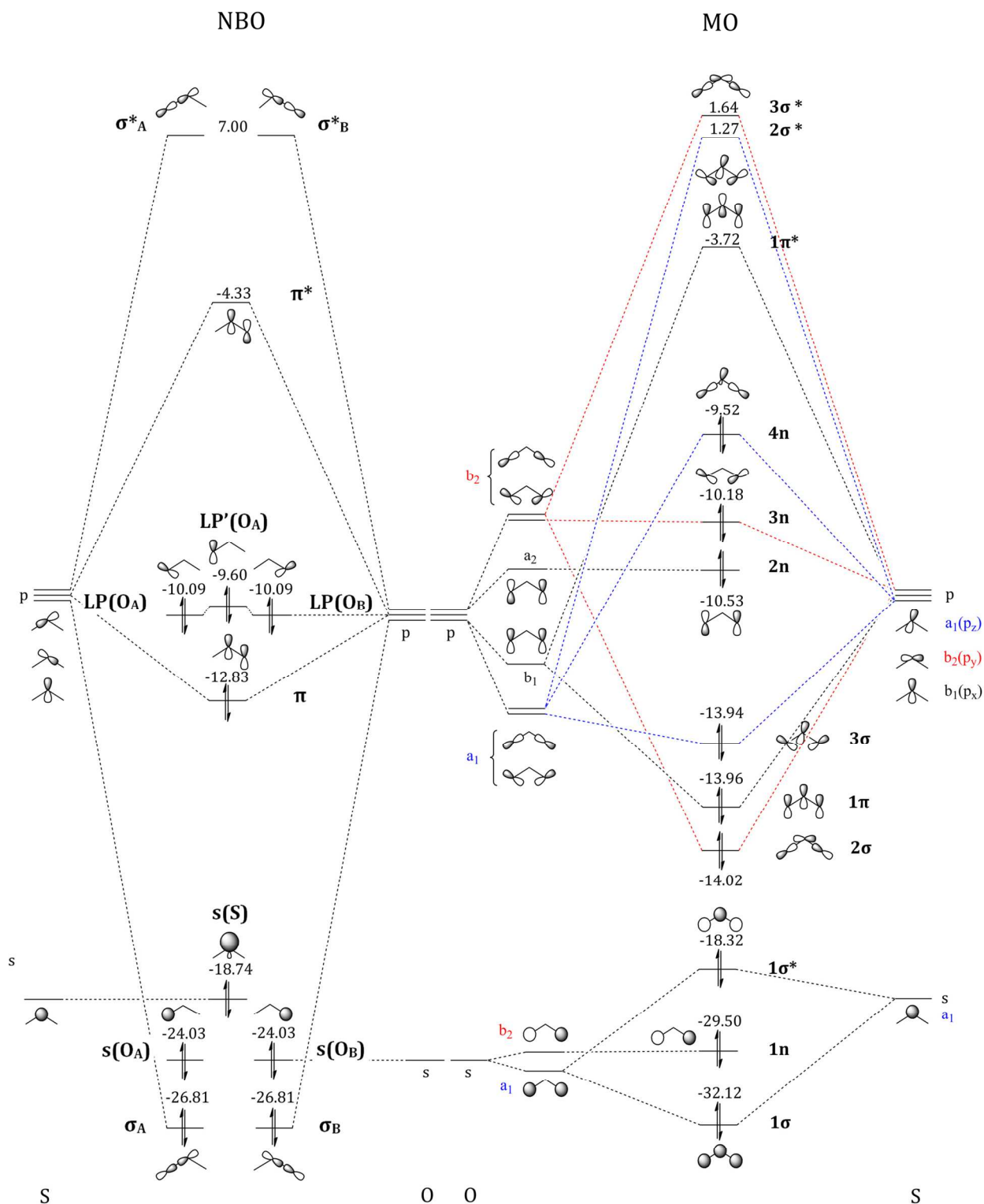
Figure 1. The diagram of natural bond orbitals (*left*) and canonical MOs (*right*). All calculated energies are in eV (PBE0/TZVP/ZORA).

NBO

MO
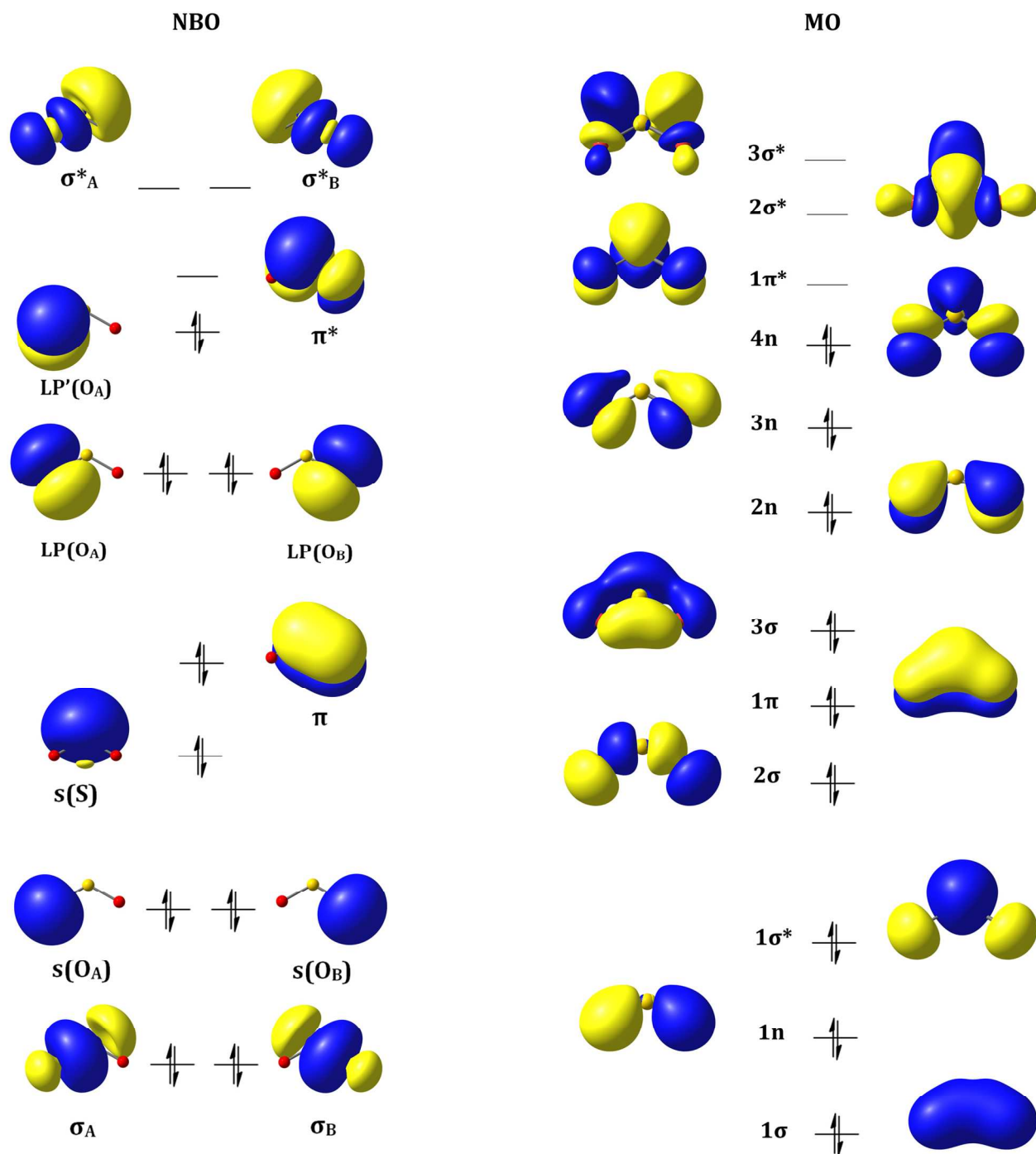
Figure 2. The NBO (*left*) and MO (*right*) diagrams for SO_2 (PBE0/TZVP/ZORA).

SO$_2$ as an Acceptor

Geometries. Geometry optimizations of the model complexes [L(CH$_3$)Pt·(SO$_2$)] and

[L'(CH$_3$)Ir·(SO$_2$)] (L and L' are simplified tridentate pincer ligand depicted in Scheme 2, real

substituents at N are replaced by hydrogens), followed by harmonic frequency calculations,

revealed that all of these compounds (Fig. 3a and b) correspond to minima on their

potential energy surfaces (PES). Calculated parameters for the Pt-based compounds (Table

1) are in reasonable agreement with available experimental data.[11] Complex with an

iridium center (and X=N), previously proposed as better candidate for being electron donor

in adducts with molecular I$_2$,[7] shows a shorter M–S bond (2.32 Å *vs.* 2.48 Å for isoelectronic

Pt-derivative), which may indicate stronger interaction. Linear complexes of d^{10} late

transition metals (Pt(0) and Pd(0) here) also form stable (here means corresponding to

local minima on their PES) adducts with SO$_2$ (Fig. 3c); calculated geometrical parameters

are in a good agreement with experimental values.[16] No significant differences were found

between complexes of platinum and palladium (Table 2). Interestingly, the Pt–S bond

length is longer in the adduct of Pt(II) (2.48 Å) than that in complexes of Pt(0) (2.36 Å),

which may also be a consequence of stronger bonding.
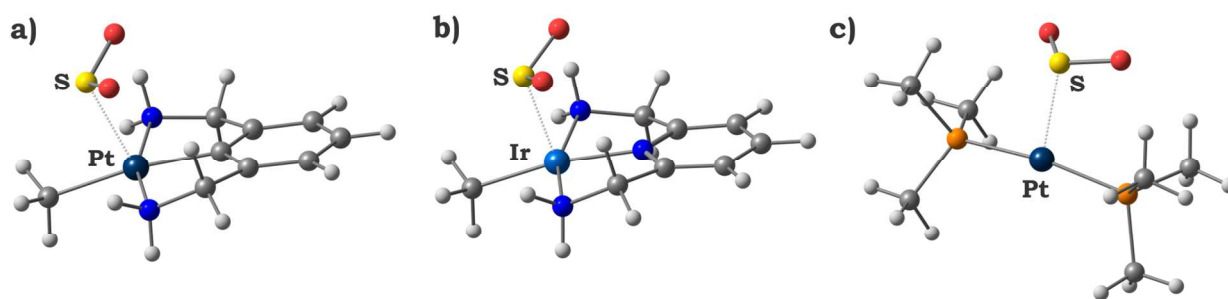
Figure 3. Opitmized equilibrium geometries (PBE0/TZVP/ZORA) for: (a) [L(CH$_3$)Pt·(SO$_2$)],

(b) [L'(CH$_3$)Ir·(SO$_2$)], and (c) [(P(CH$_3$)$_3$)$_2$Pt·(SO$_2$)] (isostructural to Pd(0)-based adduct,

presented in SI). Red, orange, and blue colors designate oxygen, phosphorus, and nitrogen atoms, respectively.

In all cases, the SO_2 molecule is attached to the metal center in the bent coordination mode. The angle between plane of SO_2 and M–S bond vector (∠M-plane in Table 1, see details in SI) was found to be 108° and 115° for M=Pt and Ir, respectively. This parameter for complexes $[(P(CH_3)_3)_2M·(SO_2)]$ is of the same magnitude (117° for M=Pt, 119° for M=Pd). As one might expect, the S–O bond became elongated in these compounds (Table 2) by comparison with unperturbed SO_2 (Table 1). The longest S–O bond corresponds to the shortest M–S bond as in the case of $[L'(CH_3)Ir·(SO_2)]$.

Table 1. Selected geometrical parameters of SO_2 adducts with van Koten complexes (PBE0/TZVP/ZORA).[a]

Parameter	SO_2	$[L(CH_3)Pt]$	$[L'(CH_3)Ir]$	$[L(CH_3)Pt·(SO_2)]$		$[L'(CH_3)Ir·(SO_2)]$
				Calc.	Exp.[d]	
M^b–S				2.48	2.48-2.61	2.32
M–C		2.13	2.09	2.14	1.92-1.95	2.09
M–Y^b		1.96	1.94	1.98	-	2.00
S–O	1.46			1.49	1.43-1.47	1.53
∠M–plane[c]				108°	114°-116°	115°
∠C–M–Y^b		180°	179°	171°	173°-177°	171°
∠C–M–S				84°	90°-103°	93°

[a] All bond lengths are in angstroms. [b] M=Pt for Y=C, M=Ir for Y=N [c] This parameter designates the angle between M–S vector and plane formed by three atoms of SO_2. [d] Since there are multiple experimental crystal structures of SO_2 adducts with Pt(II) square-planar complexes,[11] the range of observed geometrical parameters is given, when possible.

Table 2. Selected geometrical parameters for adducts [(P(CH$_3$)$_3$)$_2$M·(SO$_2$)] (M=Pt(0), Pt(0)) (PBE0/TZVP/ZORA).[a]

Parameter	[(P(CH$_3$)$_3$)$_2$Pt]	[(P(CH$_3$)$_3$)$_2$Pd]	[(P(CH$_3$)$_3$)$_2$Pt·(SO$_2$)]	[(P(CH$_3$)$_3$)$_2$Pd·(SO$_2$)]
M–S			2.36	2.35
M–P	2.25	2.27	2.30	2.33
S–O			1.50	1.49
∠M–plane			117°	119°
∠P–M–P	174°	177°	169°	167°
∠P–M–S			96°	97°

[a] All bond lengths are in angstroms. [b] M designates the metal center. [c] The bond length is the average value.

The Nature of M–(SO$_2$) Bonding in [L(CH$_3$)Pt·(SO$_2$)] and [L'(CH$_3$)Ir·(SO$_2$)]

NBO analysis. The first step in our detailed analysis of the bonding between the SO$_2$ molecule and a metal fragment was the quantification of donor-acceptor interactions within the framework of the NBO approach. In this technique, the complete picture of donor-acceptor interactions can be obtained by careful examining possible interactions between filled (donor) Lewis-type NBOs and empty (acceptor) non-Lewis NBOs, evaluating their energetic importance by using second-order perturbation theory in the NBO basis (hereafter $E^{(2)}_{i \rightarrow j}$). These interactions are usually referred to as delocalization corrections to the 0th-order natural Lewis structure due to the loss of occupancy from localized NBOs.

From a previous study,[7] it is known that the reactivity of square-planar Pt(II) complexes, like those extensively used by the group of van Koten,[11] at the axial position of the metal center can be of two types: (*i*) the metal center behaves as an acceptor via an empty Lewis Acidic Orbital (LAO) localized on the Pt, and/or (*ii*) as a donor by using doubly

occupied d_z^2 orbital. In both cases, the formation of σ-type bonding is expected. The outcomes of an NBO perturbation analysis are summarized in Table 3.

Table 3. Results of NBO analysis of donor-acceptor interaction in $[L(CH_3)Pt·(SO_2)]$ and $[L'(CH_3)Ir·(SO_2)]$ (in kcal/mol, PBE0/TZVP/ZORA).

Parameter	$[L(CH_3)Pt·(SO_2)]$	$[L'(CH_3)Ir·(SO_2)]$
	$M^a{\rightarrow}SO_2$	
$d_z^2(Pt){\rightarrow}LAO(S)$	211	-
	$SO_2{\rightarrow}M^a$	
$LP(S)^c{\rightarrow}LAO(M)^c$	10	7
	$N^d{\rightarrow}M^a$	
$LP(N(1))^b{\rightarrow}LAO(M)^c$	141	157
$LP(N(1))^b{\rightarrow}\sigma^*(C–M)$	20	
$LP(N(2))^b{\rightarrow}LAO(M)^c$	142	157
$LP(N(2))^b{\rightarrow} \sigma^*(C–M)$	20	
$E_{bonding}^e$	-24	-50

[a] M designates the metal fragment. [b] LP is the localized lone pair of the donor atom (different for each donor). [c] LAO is the available empty Lewis acceptor orbital of Pt(II) center. [d] N(1) and N(2) are the nitrogen atoms in the pincer ligand. [e] The bonding energies $E_{bonding} = \Delta E_{adduct} - \sum(\Delta E_{fragments})$, where ΔE_{adduct} and $\Delta E_{fragments}$ are energies of adducts and separately optimized fragment, respectively.

The NBO analysis (Table 3) shows that the M→(SO$_2$) term (SO$_2$ acts as an acceptor) clearly dominates over the (SO$_2$)→M one (SO$_2$ plays a role of a donor) in $[L(CH_3)Pt·(SO_2)]$. In contrast to the adduct of the same metal fragment with molecular I$_2$ (also acting as an acceptor), for which three different components of M→(I$_2$) contribution were found,[7] only one notable component of the M→(SO$_2$) contribution was observed. This component

represents a donation from $d_z{}^2$(Pt) to the empty LAO mostly localized on the sulfur atom of SO$_2$ molecule (see Fig. 4a for graphical representation of the NBOs involved). It is interesting to note here that LAO(S) corresponds to an almost ideal p_x-orbital of the sulfur atom and is slightly different from the corresponding orbital of unperturbed SO$_2$ (Fig. 2 *left*). Quantification of this bonding in terms of NBO perturbation analysis revealed a very large stabilization of 211 kcal/mol. This is dramatically larger than that for previously studied adducts of I$_2$ (total M→(I$_2$) contribution is equal to 38 kcal/mol[7]). For comparison, a similar analysis was performed for interactions between the nitrogen atoms of the pincer ligand and Pt(II) (Table 3). In spite of being of different nature (dominated by ligand→M or classical donor contribution), these interactions provide a good reference for energetic evaluations calculated by perturbation theory within the NBO basis. A detailed picture of this bonding in terms of NBO was previously considered.[7] These interactions are much stronger than that between the metal fragment and I$_2$ in [L(CH$_3$)Pt·(I$_2$)], but only *ca.* 60 kcal/mol weaker than between the same metal fragment and SO$_2$ in [L(CH$_3$)Pt·(SO$_2$)] (Table 3). It unambiguously indicates that the SO$_2$ molecule is a significantly stronger acceptor than molecular I$_2$ in the same environment.
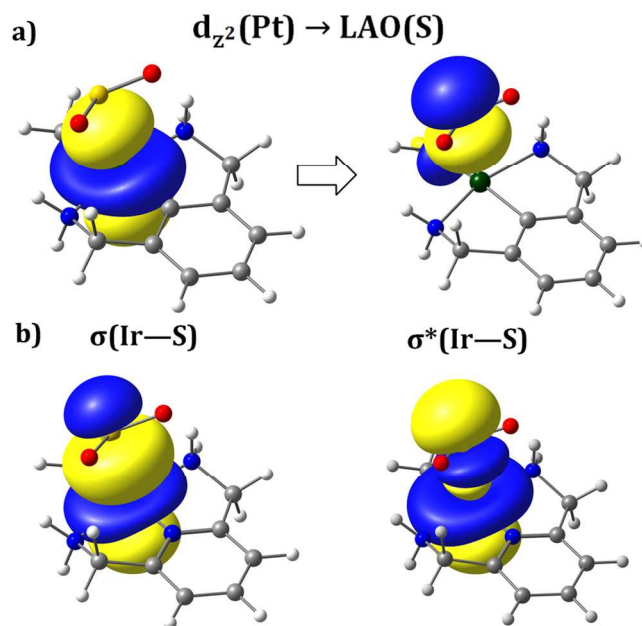
Figure 4. (*a*) The major contribution to the M→(SO₂) interaction in NBO analysis of [L(CH₃)Pt·(SO₂)]; (*b*) resulting bonding and anti-bonding NBOs in the case of [L'(CH₃)Ir·(SO₂)] (PBE0/TZVP/ZORA).

As Table 3 shows, there is a minor contribution from (SO₂)→M donation, constituting ~5% of the total attraction between SO₂ and the metal fragment as estimated by $E^{(2)}$. The major component of this contribution is the electron transfer from the LP(S) localized on the sulfur atom to the LAO(Pt) (Fig. 5), which is an empty metal-based NBO with s and d-character (~80% of s-character).
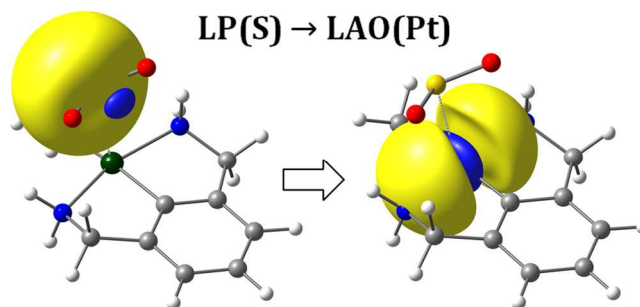
Figure 5. The major contribution to the $SO_2 \rightarrow M$ term interaction in NBO analysis (PBE0/TZVP/ZORA).

The bond between SO_2 and Ir-based metal fragment was found to be even stronger as evaluated by the total bond dissociation energy (or bonding energy). This parameter characterizes the whole spectrum of possible interactions between specified fragments and was calculated to be equal to -24 kcal/mol for $[L(CH_3)Pt \cdot (SO_2)]$ and -50 kcal/mol for $[L'(CH_3)Ir \cdot (SO_2)]$. This finding correlates with shorter M–S bond in iridium complex (Table 1). However, the high strength of the bond prevented the use of perturbation theory. Instead, the NBO technique provides a description of this interaction in terms of localized bonding and anti-bonding NBOs (or polar covalent bond, Fig. 4b). Subsequent decomposition of this bonding NBO shows that it is constructed by two hybrid orbitals (NHOs, Fig. 6) localized on sulfur and iridium atoms, respectively:

$$NBO = 0.79 \cdot h(Ir) + 0.61 \cdot h(S) = 63\% h(Ir) + 37\% h(S)$$

where $h(Ir)$ has 84% of $d_{z^2}(Ir)$ and 15% of s-orbital, whereas $h(S)$ is mainly formed by p_x-orbital of S (94%) with small (~6%) contribution s-orbital. The corresponding anti-bonding orbital (Fig. 4b *right*) is represented by opposite combination of these NHOs, with larger contribution from SO_2 part. It is also important to note that the target NBO covers 98% of the Natural Localized MO (NLMO). NLMOs correspond to the first step in

diagonalization of the density matrix (MO→NLMO). A Slater determinant of NLMOs is equivalent to the determinant of the wavefunction of the canonical MOs. Hereafter, for all systems considered, the NBO description of a target orbital corresponds to >95% of a NLMO and, thus, can be reliably used to clarify the nature of the bonding.

NHO(Ir)   NHO(S)
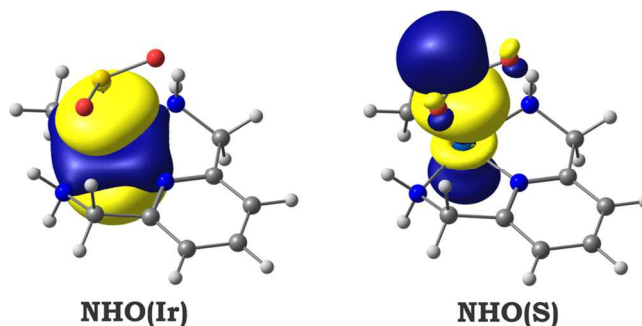
Figure 6. Two NHOs which take part in formation of the bonding NBO in [L'(CH$_3$)Ir·(SO$_2$)] (PBE0/TZVP/ZORA).

As in [L(CH$_3$)Pt·(SO$_2$)], the contribution from (SO$_2$)→M type of interaction to the total attraction in the Ir-based system was found to be minor (Table 3) and of exactly the same nature (Fig. 5).

Such a strong donor-acceptor interaction in the target systems, which even led to the formation of the polar covalent bond in the case of [L'(CH$_3$)Ir·(SO$_2$)], has an immediate effect on atomic charge distribution and bond orders. The calculated Wiberg bond orders and atomic charges for the model adducts are collected in Figure 7. As one might expect, the donor-acceptor interaction between the SO$_2$ molecule and metal fragment led to notable increase of positive charge on the metal center (from +0.52 to +0.64 for M=Pt(II) and from +0.15 to +0.33 for M=Ir(I)). The opposite trend was expectedly observed for the

charge of the sulfur atom of SO_2. The charge of sulfur (+1.52 in unperturbed SO_2) decreases

due to electron transfer from the metal center in the adducts (to +1.45 in [L(CH_3)Pt·(SO_2)]

and to +1.37 in [L'(CH_3)Ir·(SO_2)]). It should be noted that all changes are more pronounced

for the Ir-based compound. This agrees well with the previous observation of a larger

bonding energy between SO_2 and the metal fragment in [L'(CH_3)Ir·(SO_2)] in comparison

with that for the isoelectronic Pt(II)-complex (Table 3). Another support arrives from the

M–S bond order, which is equal to 0.36 for [L(CH_3)Pt·(SO_2)] and 0.64 for [L'(CH_3)Ir·(SO_2)].
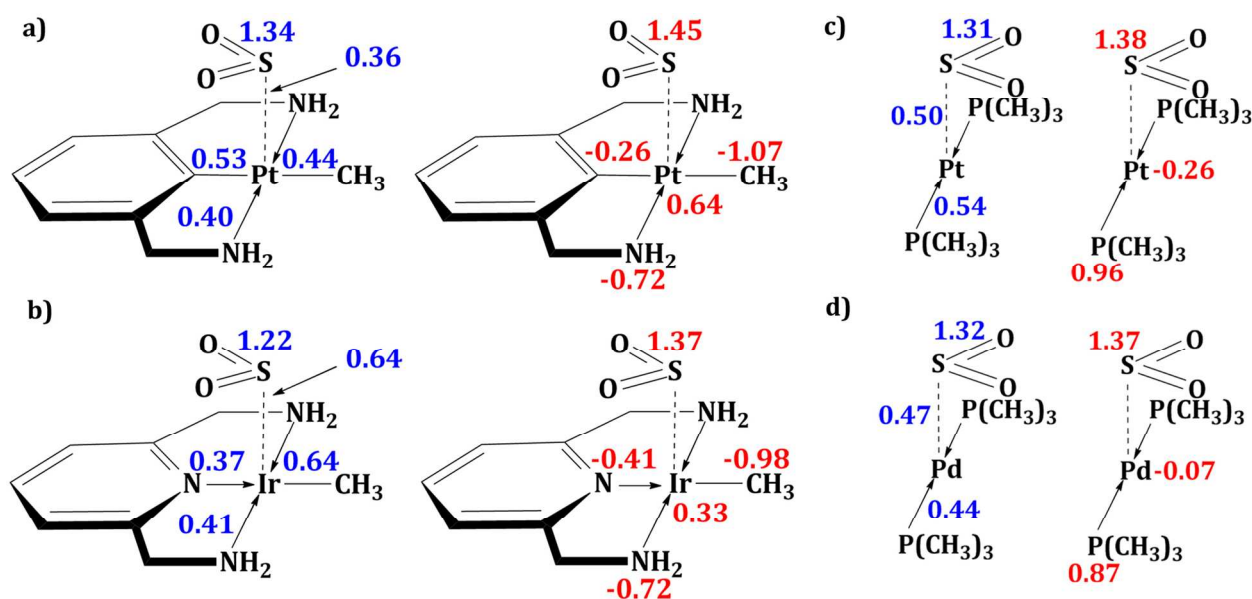
Figure 7. The Wiberg bond orders and NBO charges for model adducts (PBE0/TZVP/ZORA). The blue color is for bond orders, the red is for charges.

Subsequent *EDA analysis* (Table 4) revealed the importance of both contributions to

the bonding, namely ΔE_{orb} (considered as covalent part) and ΔE_{elstat} (usually accepted as

ionic part). The covalent contribution is ~10 kcal/mol smaller than the ionic one for all

compounds of the series. Interestingly, a significant growth of the orbital component when

going from systems with M=Pt(II) to those with M=Ir(I) (-67 kcal/mol $vs.$ -141 kcal/mol,

respectively) is complemented by an analogous increase of the electrostatic term (-74

kcal/mol $vs.$ -152 kcal/mol). However, the ratio between the bonding components remains

the same. The repulsive term (ΔE_{Pauli}) also follows the same direction (from +116 kcal/mol

for [L(CH$_3$)Pt·(SO$_2$)] to +236 kcal/mol for [L'(CH$_3$)Ir·(SO$_2$)]). Thus, the growth of attraction

in the target systems is augmented by an increase of the repulsive term. Similar tendencies

were observed previously in the case of adducts of molecular I$_2$.[7] Another consequence of

strengthening the M–S bond is an enlargement the preparation energy, which goes from +6

kcal/mol for M=Pt(II) to +13 kcal/mol for M=Ir(I).

Table 4. Results of EDA analysis of M–(SO$_2$) bonding (in kcal/mol, PBE0/TZ2P/ZORA).

Parameter	[L(CH$_3$)Pt·(SO$_2$)]	[L'(CH$_3$)Ir·(SO$_2$)]	[(P(CH$_3$)$_3$)$_2$Pt·(SO$_2$)]	[(P(CH$_3$)$_3$)$_2$Pd·(SO$_2$)]
ΔE_{int}	-25	-57	-34	-31
ΔE_{elstat}	-74 (52%)[a]	-152 (54%)[a]	-104 (53%)[a]	-83 (56%)[a]
ΔE_{orb}	-67 (48%)[a]	-141 (46%)[a]	-92 (47%)[a]	-74 (44%)[a]
ΔE_{Pauli}	+116	+236	+162	+126
$-D_e$[b]	-19	-44	-28	-24
ΔE_{prep}	+6	+13	+6	+7

[a] The percentages are the contributions of the respective terms to the sum of ΔE_{elstat} + ΔE_{orb}. [b] D_e is
the dissociation energy of the interaction between the fragments. The bonding energy, $E_{bonding}$ = $-D_e$ =
ΔE_{int} + ΔE_{prep}. $-D_e$ is negative, when the molecule is bound.

The Nature of M–(SO$_2$) Bonding in Complexes of d^{10} Metals.

NBOs of linear [(P(CH$_3$)$_3$)$_2$Pt] and [(P(CH$_3$)$_3$)$_2$Pd]. The NBO localization scheme produces five well-localized d-orbitals for the metal center (Fig. S4-S5). Considering symmetry restrictions, one can select from this set three potentially available donor orbitals for interaction with the SO$_2$-acceptor. Two other d-orbitals are not suited for interaction with available acceptor orbital of SO$_2$, which is mostly formed by sulfur p$_x$-orbital.

      NBO analysis of the bonding in [(P(CH$_3$)$_3$)$_2$M·(SO$_2$)], where M=Pt(0), Pd(0). The shorter M–S bond in the adducts of linear organometallic fragments with SO$_2$ (in comparison with Pt(II)-based adducts) may be indicative a stronger bonding. Indeed, the total bonding energy was calculated to be significantly larger (-31 kcal/mol and -30 kcal/mol for M=Pt(0) and Pd(0), respectively), than those in [L(CH$_3$)Pt·(SO$_2$)] (Table 3). Furthermore, the bonding situation cannot be described by perturbation theory of the second order due to its high strength, analogous to what was previously seen in the case of [L'(CH$_3$)Ir·(SO$_2$)]. Instead, the description in terms of localized bonding and anti-bonding NBOs was provided (Fig. 8). The bonding NBO can further be represented as a result of interaction of two hybrid orbitals (Fig. 9):

$$NBO = 0.83 \cdot h(\text{Pt}) + 0.56 \cdot h(\text{S}) = 68\% h(\text{Pt}) + 32\% h(\text{S})$$

where h(Pt) has 74% of d$_{z^2}$(Pt) and 26% of s-orbital, whereas h(S) is mainly formed by p$_x$-orbital of S (96%) with small (~3%) contribution s-orbital. One can note a larger contribution of the s-orbital to the NHO(Pt(0)) in comparison with the NHO(Ir(I)) in the iridium-based adduct. The corresponding anti-bonding NBO (Fig. 8 *right*) is formed by reversed combination of the above mentioned NHOs. No difference was found between adducts of Pt(0) and Pd(0) (see SI for details).

σ(M—S)   σ*(M—S)
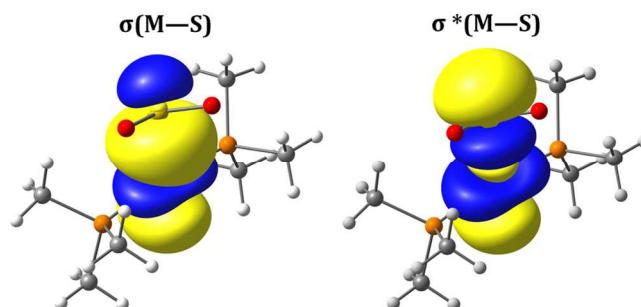
Figure 8. The bonding (*left*) and anti-bonding (*right*) NBOs in the case of [(P(CH₃)₃)₂Pt·(SO₂)] (PBE0/TZVP/ZORA, analogous orbitals for the Pd-based adduct can be found in SI).

NHO(Pt)   **NHO(S)**
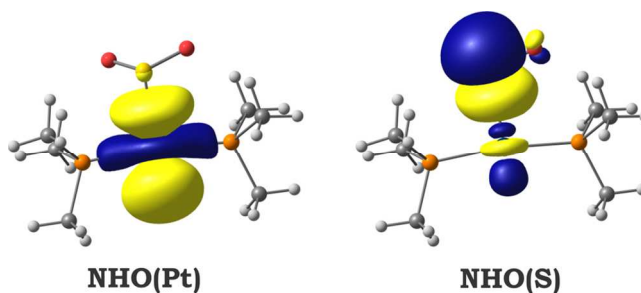
Figure 9. Two NHOs, which take part in formation of the bonding NBO in [(P(CH₃)₃)₂Pt·(SO₂)] (PBE0/TZVP/ZORA, analogous orbitals for the Pd-complex can be found in SI).

Atomic charge distribution and Wiberg bond orders (Fig. 7, *c* and *d*) are in full agreement with NBO picture of the bonding in target molecules as well as with their geometric parameters. So, the coordination of a SO_2 molecule resulted in a decrease of negative charge on the metal center (from -0.55 to -0.26 and from -0.33 to -0.07 for Pt and Pd, respectively). It supports the general conclusion about SO_2 behaving as a strong acceptor in [(P(CH₃)₃)₂M·(SO₂)] (M=Pt(0), Pd(0)). A shorter M–S bond (Table 1) agrees

with higher bond order (Fig. 7) in comparison to [L(CH$_3$)Pt·(SO$_2$)]. However, the bond order was found to be smaller than in the case of [L'(CH$_3$)Ir·(SO$_2$)], where the M–S bond was even shorter. These findings are in line with the trend in total bonding energy, which was calculated to be the highest for Ir-based adduct. Thus, one can see the nice correlation between bond strength, bond order and bond length: the shorter the bond, the higher the bond order and the larger the bonding energy.

EDA analysis of the bonding revealed essentially the same bonding pattern in [(P(CH$_3$)$_3$)$_2$M·(SO$_2$)] as in the case of [L(CH$_3$)Pt·(SO$_2$)] and [L'(CH$_3$)Ir·(SO$_2$)] (Table 4). Both contributions, ΔE_{orb} and ΔE_{elstat}, follow the same trend as the total bond dissociation energy (-D_e): they are larger than that for Pt(II)-based complex and smaller than that for Ir-based one. With the same balance between covalent and ionic parts. The same is true for the repulsive ΔE_{Pauli} term and preparation energy (ΔE_{prep}).

SO$_2$ as a Donor

Geometries. In the next step of this investigation, we switched to organometallic fragments that have a reputation of being pronounced Lewis Acids, namely, paddle-wheel [Rh$_2$(O$_2$CCF$_3$)$_4$][7, 20] and classic square-pyramidal [M(CO)$_5$], M=Cr, W.[17,18] Geometry optimization of the model complexes [Rh$_2$(O$_2$CCF$_3$)$_4$·(SO$_2$)] and [M(CO)$_5$·(SO$_2$)], followed by harmonic frequency calculations, indicated that all of these adducts correspond to minima on their PES (Fig. 10). The calculated parameters are collected in Table 5 and Table 6.
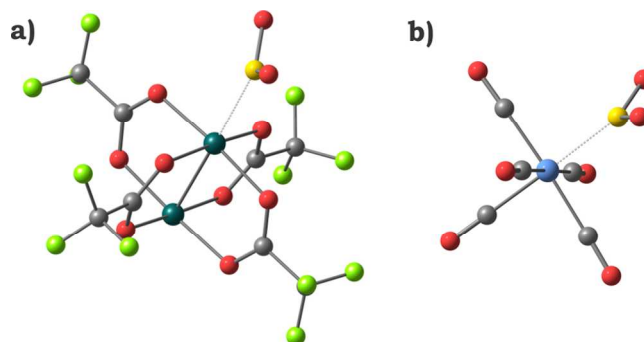
Figure 10. The optimized equilibrium geomtries for model complexes (a) $[Rh_2(O_2CCF_3)_4 \cdot (SO_2)]$ and (b) $[Cr(CO)_5 \cdot (SO_2)]$ (PBE0/TZVP/ZORA, for isostructural W-analog see SI).

Table 5. Selected calculated geometrical parameters of $[Rh_2(O_2CCF_3)_4 \cdot (SO_2)]$ (PBE0/TZVP/ZORA).[a]

Parameter	$[Rh_2(O_2CCF_3)_4]$	$[Rh_2(O_2CCF_3)_4 \cdot (SO_2)]$
Rh–Rh	2.38	2.40
Rh–S		2.42
S–O		1.45
∠Rh–Rh–S		178°
∠O–S–O		121°
∠M–plane[b]		178°

[a] All bond lengths are in angstroms; angles are in degrees. [b] This parameter designates the angle between M–S vector and plane formed by three atoms of SO_2.

Table 6. Selected Calculated Geometrical Parameters of $[M(CO)_5 \cdot (SO_2)]$, where M=Cr, W (PBE0/TZVP/ZORA).[a]

Parameter	$[Cr(CO)_5]$	$[W(CO)_5]$	$[Cr(CO)_5 \cdot (SO_2)]$	$[W(CO)_5 \cdot (SO_2)]$
M–C[b]	1.90	2.04	1.90	2.45
M–C'[c]	1.83	1.93	1.88	2.01

M–S	2.23	2.38
S–O	1.46	1.46
∠O–S–O	118°	118°
∠M–plane	179°	178°

[a] All bond lengths are In angstroms; angles are in degrees. [b] This value is an average over the four M–C bonds between metal center and equatorial CO ligands. [c] This parameter corresponds to the M–C bond with axial CO ligand.

In all cases, the axial SO_2 molecule is attached to the metal center in linear coordination mode with angle ∠M–plane being close to 180°. This geometry is in sharp contrast with what was found in the case of donor metal fragments as well as pure organic donor molecules. The bonding mode in both $[Rh_2(O_2CCF_3)_4 \cdot (SO_2)]$ and $[M(CO)_5 \cdot (SO_2)]$ matches the expectations for maximized interaction between the lone pair of SO_2 (thus, acting as a donor) and the available unoccupied orbital of $[Rh_2(O_2CCF_3)_4]$ and/or $[M(CO)_5]$ (playing the role of an acceptor). The Rh–Rh bond in the adduct with sulfur dioxide was found to be elongated by 0.02Å in comparison with that in unperturbed dimetal complex (Table 5). Usually, this bond is indicative of the strength of donor-acceptor interaction between the dirhodium fragment and the donor molecule.[20] If one agrees with this, molecular I_2 seems to be a stronger donor than SO_2, because of the elongated Rh–Rh bond in its corresponding adduct (2.45Å *vs.* 2.40Å). At the same time, the S–O bond remains essentially unchanged in all adducts with Lewis acidic metal fragments (Table 5 and Table 6). These findings are in line with donor behavior of the SO_2 molecule via the lone pair of sulfur atom, which only slightly involved in bonding with oxygens (Fig. 1 and Fig. 2).

The Nature of M–(SO$_2$) Bonding in [Rh$_2$(O$_2$CCF$_3$)$_4$·(SO$_2$)] and [M(CO)$_5$·(SO$_2$)] (M=Cr,W)

We have started an analysis of the bonding between metal fragment and SO$_2$ with detailed consideration of donor-acceptor interactions within a *NBO framework*. The electronic structure of the parent organometallic complexes [Rh$_2$(O$_2$CCF$_3$)$_4$] and [M(CO)$_5$] (M=Cr, W) in terms of NBOs were previously considered in detail.[7,18] The NBO picture of unperturbed SO$_2$ was detailed previously in this paper. So, we now proceed with consideration of the adducts. The dominant donor-acceptor interactions emerging from the NBO analysis are collected in Table 7.

Table 7. Donor-acceptor interactions in [Rh$_2$(O$_2$CCF$_3$)$_4$·(SO$_2$)] and [M(CO)$_5$·(SO$_2$)] (M=Cr, W) adducts, estimated by the second order NBO perturbation theory, $E^{(2)}_{i \to j}$ (in kcal/mol, PBE0/TZVP/ZORA).

Parameter	[Rh$_2$(O$_2$CCF$_3$)$_4$·(SO$_2$)]	[(Cr(CO)$_5$)·(SO$_2$)]	[(W(CO)$_5$)·(SO$_2$)]
	M^a→(SO$_2$)		
d$_{xz}$(M)→LAO(S)^b	7	148	216
	(SO$_2$)→M^a		
LP(S)^c→σ*(Rh–Rh)	54	-	-
$E_{bonding}$^{d}	-8	-25	-27

^{a} M designates the metal fragment. ^{b} LAO is the available empty Lewis acceptor orbital of SO$_2$ molecule. ^{c} LP is the localized lone pair of the donor atom (different for each donor). ^{d} The bonding energies $E_{bonding}$ =ΔE_{adduct} - $\sum(\Delta E_{fragments})$, where ΔE_{adduct} and $\Delta E_{fragments}$ are energies of adducts and separately optimized fragment, respectively.

From previous studies, it is known that dirhodium paddle-wheel complex shows characteristic Lewis acid behavior through the low-lying empty σ*-orbital mainly localized on the dimetal core. At the same time, there are two degenerate doubly occupied MOs of π-

symmetry, formed mostly by d-orbitals of the metal centers. These orbitals are relatively high-lying and could participate in donor-acceptor interactions with suitable acceptor LAO of appropriate symmetry. However, such an interaction is not expected to be strong. This is indeed what was found in the case of $[Rh_2(O_2CCF_3)_4 \cdot (SO_2)]$ adducts. In contrast to previously considered complexes with a bent coordination mode of the SO_2 molecule, the ligand→metal type of interaction is dominating over the metal→ligand one (Table 7). The nature of the interaction unambiguously corresponds to the donation from the lone pair of SO_2 to $\sigma^*(Rh–Rh)$ orbital of $[Rh_2(O_2CCF_3)_4]$ (Fig. 11a). the metal-to-ligand contribution was found to be much smaller (7 kcal/mol *vs.* 54 kcal/mol, respectively). The nature of this term can be clearly described as donation from d_{xz} orbital of dimetal core to the LAO(S) (Fig. 12a). Interestingly, the set of doubly occupied π- and π^*-MOs in $[Rh_2(O_2CCF_3)_4]$ is transformed to two almost ideal d-orbitals, independently localized on the two metal centers in terms of the NBO technique.
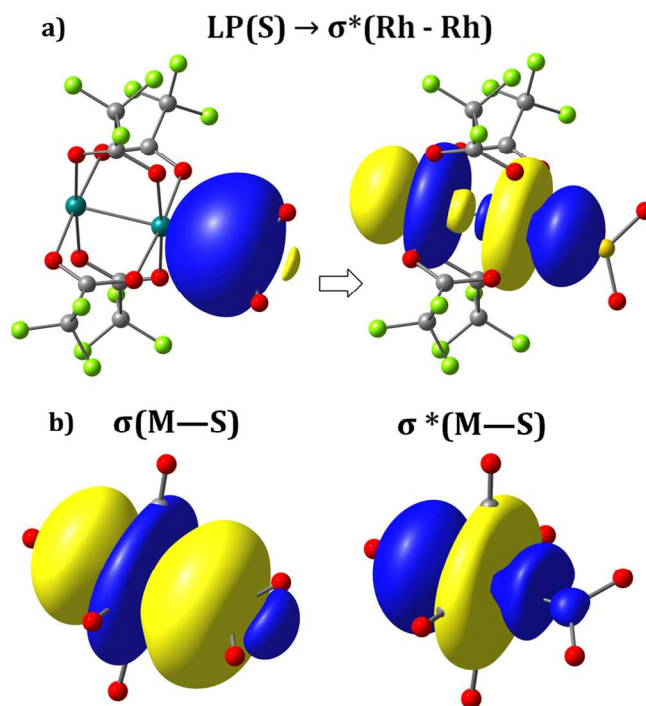
Figure 11. (*a*) The major contribution to $(SO_2)\rightarrow M$ interaction in $[Rh_2(O_2CCF_4)\cdot(SO_2)]$, and

(*b*) bonding and anti-bonding NBOs in $[M(CO)_5\cdot(SO_2)]$ (M = Cr, W) (PBE0/TZVP/ZORA).
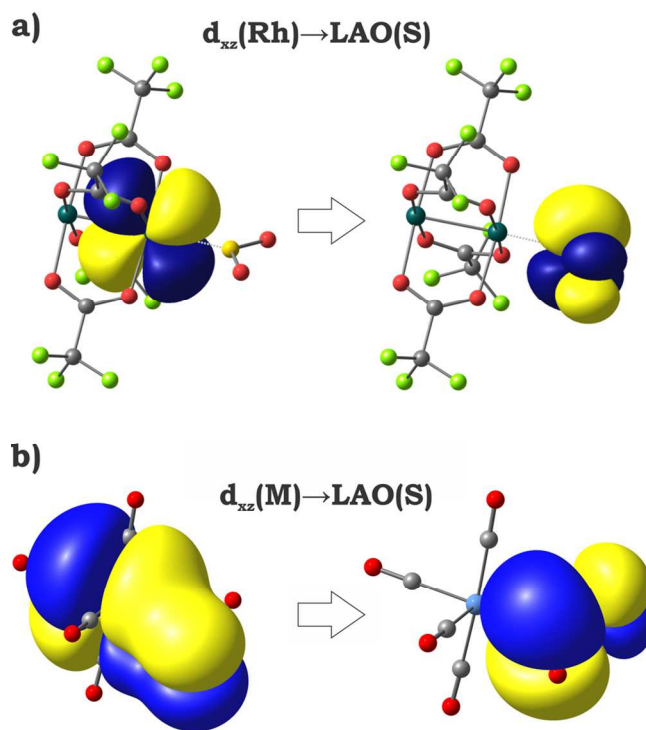
Figure 12. The major contribution to M→(SO$_2$) interaction in (*a*) [Rh$_2$(O$_2$CCF$_4$)·(SO$_2$)] and (*b*) [M(CO)$_5$·(SO$_2$)] (M = Cr, W) (PBE0/TZVP/ZORA).

Adducts [M(CO)$_5$·(SO$_2$)] (M = Cr, W) also show the same nature of interaction between the metal fragment and sulfur dioxide, in which the (SO$_2$)→M term dominates over the M→(SO$_2$) one. The bonding can be described as a polar covalent bond rather than a donor-acceptor interaction (see bonding and anti-bonding NBOs in Fig. 11b), analogous to what we have seen in complexes [L'(CH$_3$)Ir·(SO$_2$)], [(PH$_3$)$_2$M·(SO$_2$)] (M=Pd(0), Pt(0)), and [^{Me}NHC·(SO$_2$)]. The bonding NBO (Fig. 11b) can be considered as result of mixing of two NHOs (Fig. 13), localized on different fragments:

$$NBO = 0.52 \cdot h(Cr) + 0.86 \cdot h(S) = 27\% h(Cr) + 73\% h(S)$$

where $h(Cr)$ has 68% of d-character and 32% of s-orbital, whereas $h(S)$ is formed by s-orbital (52%) and p-orbital (48%) of S. Thus, the major contribution to the bonding NBO

comes from the occupied NHO (lone pair) of the SO_2 molecule (Fig. 13 *right*). The anti-bonding NBO corresponds to an out-of-phase combination of these NHOs and, thus, is mainly formed by the empty NHO localized on the metal fragment (Fig. 13 *left*). Very similar bonding was observed for W-based adducts (see SI for details).

Importantly, in adducts $[M(CO)_5 \cdot (SO_2)]$ (M = Cr, W), the M→(SO_2) contribution was found to be significant (Fig. 12b, Table 7). Albeit being of the same nature as in $[Rh_2(O_2CCF_4) \cdot (SO_2)]$ (Fig. 12a), this contribution has a much larger magnitude and is close to that in the $[L(CH_3)Pt \cdot (SO_2)]$ system, in which metal-to-ligand term is leading (Table 3). Hence, in such adducts, the SO_2 molecule exhibits donor and acceptor properties (predominantly donor) rather than just being a pure donor.

NHO(Cr)   NHO(S)
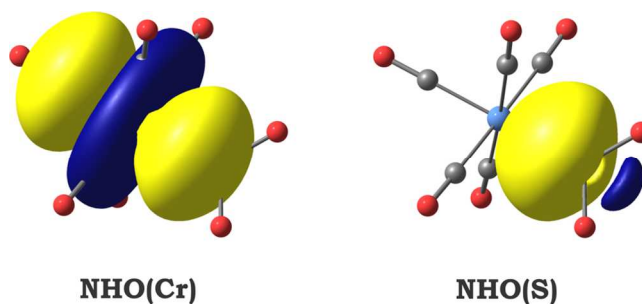
Figure 13. Two NHOs, which take part in formation of the bonding NBO in $[Cr(CO)_5 \cdot (SO_2)]$ (PBE0/TZVP/ZORA, for analogous NHOs for W-derivatives see SI).

Subsequent calculations of bond orders and atomic charges in the adducts, both $[Rh_2(O_2CCF_4) \cdot (SO_2)]$ and $[M(CO)_5 \cdot (SO_2)]$ (M = Cr, W) (Fig. 14) are in excellent agreement with our previous conclusions arrived from analysis of geometrical parameters and quantification of interactions in terms of NBO perturbation theory. So, the coordination of a SO_2 molecule to the paddle-wheel metal fragment resulted in substantial decrease of Rh–Rh

bond order and positive charges of metal centers due to an electron donation from the lone pair of the S atom to the anti-bonding σ^*(Rh–Rh) orbital (*Rh–Rh bond orders*: from 0.83 in unperturbed $[Rh_2(O_2CCF_4)]$ to 0.76 in $[Rh_2(O_2CCF_4)\cdot(SO_2)]$; *Rh-atomic charges*: from +0.93 to +0.76 and +0.86, respectively). The Rh–S bond order shows a notable value of 0.27.
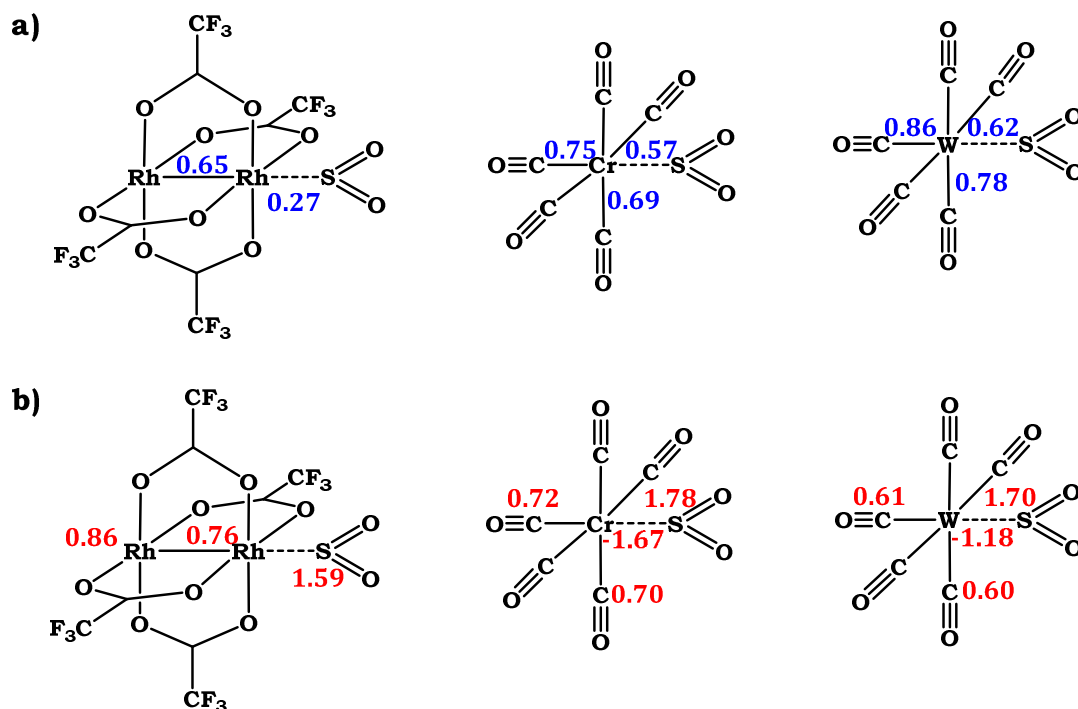
Figure 14. The Wiberg bond orders (*a*) and NBO charges (*b*) in $[Rh_2(O_2CCF_3)_4\cdot(SO_2)]$ and $[M(CO)_5\cdot(SO_2)]$ (M=Cr, W) adducts (PBE0/TZVP/ZORA). The blue is for bond orders, the red is for charges.

The same trends, even more pronounced, were shown by adducts $[M(CO)_5\cdot(SO_2)]$ (M = Cr, W). Negative charge of the metal center is increased significantly when going from unperturbed $[M(CO)_5]$ to the adduct with sulfur dioxide (from -1.02 to -1.67 for M=Cr; from

-0.63 to -1.18 for M=W). The M–S bond orders were found to be 0.57 and 0.62 for chromium and tungsten derivatives, respectively.

The positive charge of the sulfur is notably increased from +1.52 in isolated SO_2 molecule to +1.59 in $[Rh_2(O_2CCF_4)\cdot(SO_2)]$, +1.78 in $[Cr(CO)_5\cdot(SO_2)]$, and +1.70 in $[W(CO)_5\cdot(SO_2)]$, thus showing a substantial electron density depletion from the SO_2 moiety upon coordination.

The interplay between ionic and covalent components of the bonding between the organometallic Lewis acidic fragment and SO_2 (here acting as a donor), was clarified with help of *EDA analysis* (Table 8). First of all, there is a stronger donor-acceptor interaction in $[M(CO)_5\cdot(SO_2)]$ in comparison with $[Rh_2(O_2CCF_3)_4\cdot(SO_2)]$, which is immediately reflected in the magnitude of the orbital component (-58 kcal/mol and -64 kcal/mol *vs.* -35 kcal/mol, respectively), whereas, the electrostatic contribution was found to be very similar for all target adducts (Table 8).

Table 8. Results of EDA analysis of bonding in in $[Rh_2(O_2CCF_3)_4\cdot(SO_2)]$ and $[M(CO)_5\cdot(SO_2)]$ (M=Cr, W) adducts (in kcal/mol, PBE0/TZ2P/ZORA).

Parameter	$[Rh_2(O_2CCF_3)_4\cdot(SO_2)]$	$[Cr(CO)_5\cdot(SO_2)]$	$[W(CO)_5\cdot(SO_2)]$
ΔE_{int}	-8	-25	-30
ΔE_{elstat}	-26(43%)	-30(34%)	-35(35%)
ΔE_{Pauli}	53	63	69
ΔE_{orb}	-35(57%)	-58(66%)	-64(65%)
$-D_e$	-8	-24	-27
ΔE_{prep}	0	1	3

Comparison of these results with those for the systems in which SO_2 plays the role of an acceptor, revealed that all components of the bonding (attractive ΔE_{orb} and ΔE_{elstat} and repulsive ΔE_{Pauli}) are substantially larger in magnitude in the latter (Table 4). It unambiguously shows that the Lewis acidic behavior of SO_2 molecule is much more pronounced than the Lewis basic one. This is also supported by the total bond dissociation energy ($-D_e$), which was found to be larger in magnitude in the case of adducts of SO_2 as an acceptor. Interestingly, adducts with SO_2-donor possess the covalent term larger by ~10 kcal/mol than ionic contribution (Table 8), in contrast to what was observed for adducts of SO_2-acceptor (Table 4).

Adducts with Pure Organic Donors/Acceptors

The pure donor and acceptor behavior of the SO_2 molecule through the same S-atom was further supported by calculations of model adducts of sulphur dioxide with pure organic donors (Scheme 3) and acceptors like BH_3 and $B(CF_3)_3$. Geometrical parameters as well as NBO and EDA analyses of the bonding are given in Supporting Information.

Scheme 3

$C_7H_{13}N$ NH_3 $(CH_3)_3N$ ^{Me}NHC
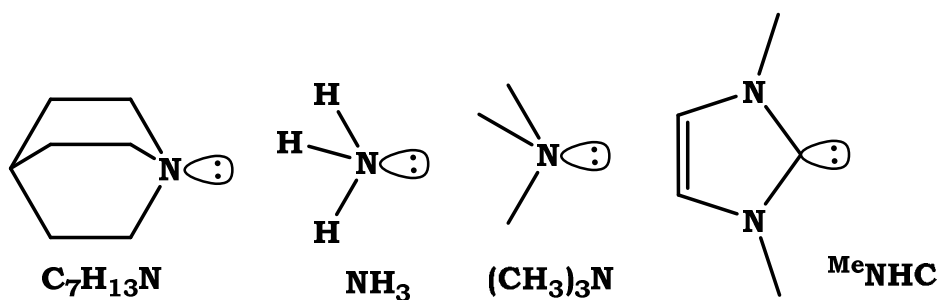
The bent coordination mode of the SO_2 moiety in complexes with donor molecules is well reproduced in all optimized equilibrium geometries (exemplified by the $[(NH_3)\cdot(SO_2)]$ compound in Fig. 15). Such adducts are well-known experimentally and their bent shape is established.[21] The trends in distances between the two interacting fragments are very similar for those in SO_2-adducts with corresponding donor organometallic fragments described above. Subsequent NBO and EDA analysis revealed exactly the same nature of the bonding between fragments, supporting our previous conclusions about SO_2 playing a role of pure acceptor. The calculated bonding energies range from -10 kcal/mol ($[(NH_3)\cdot(SO_2)]$) to -18 kcal/mol for $[(NHC)\cdot(SO_2)]$.
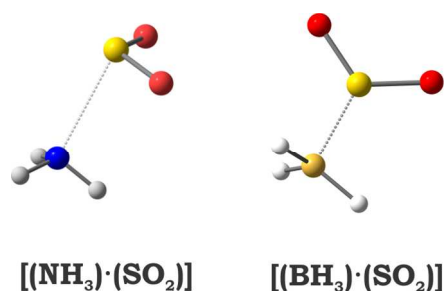
$[(NH_3)\cdot(SO_2)]$ $[(BH_3)\cdot(SO_2)]$

Figure 15. Equilibrium geometry configurations for adducts of SO_2 with (*left*) organic donor molecules (exemplified by $[(NH_3)\cdot(SO_2)]$) and (*right*) with organic acceptors (exemplified by $[(BH_3)\cdot(SO_2)]$).

At the same time, the linear coordination mode of SO_2 is well-reproduced in optimized equilibrium geometries of both $[(BH_3)\cdot(SO_2)]$ (Fig. 15) and $[(B(CF_3)_3)\cdot(SO_2)]$, with the angle between the B–S bond vector and the plane of SO_2 moiety being equal to ~180°. These finding is well-consistent with aforementioned results obtained for adducts of SO_2 (now acting as a donor species) organometallic complexes, which have a reputation

of being good acceptors. Subsequent calculations of the total bonding energies that ranges from -9 kcal/mol for $[(BH_3)\cdot(SO_2)]$ to -3 kcal/mol for $[(B(CF_3)_3)\cdot(SO_2)]$ provide an additional evidence that the Lewis acidic character of the SO_2 molecule is significantly more pronounced that the Lewis base one.

CONCLUDING REMARKS

Our detailed theoretical analysis of SO_2 adducts with organometallic fragments with d^8 or d^{10} configuration of the metal center, where sulfur dioxide occupies the fifth axial ([L(CH$_3$)Pt·(SO$_2$)] and [L'(CH$_3$)Ir·(SO$_2$)]) or the third ([(PH$_3$)$_2$M·(SO$_2$)], M=Pt(0), Pd(0)) position, allowed us to unambiguously assign the nature of this interaction. The bonding between SO_2 and metal center is best described as donor-acceptor, in which SO_2 plays a role of a strong acceptor through the low-lying empty orbital (LAO(S)) of p-symmetry. The metal fragment acts as a donor in this interaction, through an orbital mainly d_z^2 in nature. The classical $(SO_2) \rightarrow M$ interaction, in which sulfur compound acts as a donor, is very weak. The acceptor behavior of the SO_2 molecule was also supported by consideration of its adducts with pure organic donors such as amines and N-heterocyclic carbene. In spite of a high degree of similarity between complexes of donor metal fragments and these adducts, the stability of the latter as estimated by calculation of the total bonding (or bond dissociation) energy was found to be notably smaller.

Another face of reactivity of SO_2, namely, a donor behavior was analyzed in-depth in its adducts with metal fragments that have a reputation of being strong Lewis Acids such as paddle-wheel complex [Rh$_2$(O$_2$CCF$_3$)$_4$] and [M(CO)$_5$] (M = Cr, W). Consistent with linear coordination mode of the SO_2, their interaction with metal fragment(s) is best described as donor-acceptor, where sulfur dioxide behaves as a donor through the lone pair of the S atom. The metal fragment plays the role of an acceptor through the σ^*(Rh–Rh) of the dirhodium core or a hybrid orbital of [M(CO)$_5$], which is mainly formed by d_z^2-orbital of the metal center. Importantly, the donation in the reverse direction was found to be strong in the case of [M(CO)$_5$·(SO$_2$)] adducts. Thus, the SO_2 molecule acts in these complexes not only

as a good donor, but also as relatively strong acceptor. This is in contrast to what was observed for another two-faced ligand – molecular I_2, recently studied with the help of the same sets of theoretical tools.[7] For the latter, the contribution from $M \rightarrow (I_2)$ component to the total bonding in adducts with acceptor metal fragments was found negligible.

The donor behavior of the SO_2 molecule was also confirmed by the investigation of its adducts with pure organic acceptors such as BH_3 and $B(CF_3)_3$. The close resemblance between such compounds and complexes with organometallic acceptor fragments was established.

Thus, we have studied another simple molecule, SO_2, which can be considered as a two-faced ligand in organometallic chemistry, and its adducts with different donor/acceptor organic and metal fragments. The nature of interaction is supported by well-delineated geometrical signatures. However, the SO_2 molecule appeared to be a strong acceptor and relatively weak donor. This is contrast to molecular I_2, which was found to be a donor and an acceptor of approximately the same strength.

CALCULATION DETAILS

Geometry optimizations of all systems under consideration were performed with density functional theory (DFT), employing the hybrid correlation-exchange parameter-free functional of Perdew-Burke-Erzenhof (PBE0).[22] All atoms were described by a segmented all-electron relativistically contracted basis sets of triple-zeta quality augmented by polarization function (so-called SARC-TZVP basis sets), recently developed by Neese and coworkers.[23] The key feature of such an approach is complete consideration of all electrons of the model and direct accounting of relativistic corrections. Problems with

interaction between core and valence electrons, difficulties that sometimes appear when doing calculations using effective core potentials (ECP), are thus avoided.

To accelerate calculations, the resolution-of-identity (RI) algorithm was applied using the chain-of-sphere approach,[24] specifically developed recently for hybrid functionals (RIJCOSX in the ORCA[25] software terminology). This technique was found to be very efficient, with negligible loss in accuracy by comparison with standard hybrid functionals. Scalar relativistic effects have been incorporated by applying the zero-order regular approximation (ZORA). All these calculations were carried out by using the ORCA program suite (version 3.0.1).[25]

In all cases, no symmetry restrictions were applied. All calculated structures correspond to local minima (no imaginary frequencies) on the corresponding potential energy surfaces, as determined by calculation of the full Hessian matrix, followed by estimation of frequencies in the harmonic approximation.

In the next step, optimized geometries were used to get insight into the electronic structure of our target systems in terms of natural bond orbitals (NBO).[14] Bond orders quoted are those from the Wiberg formulation[26] (so-called Wiberg bond indexes) incorporated in the NBO analysis. All computations were performed with GENNBO (version 6.0) program,[27] using the converged wavefunctions generated by ORCA programs.

The bonding between metal-based fragment and sulphur dioxide was further investigated by the energy decomposition analysis (EDA) developed by Morokuma and by Ziegler and Rauk.[28] For this purpose, single-point calculations were performed by the ADF program package[29] with the same functional. All atoms were described by uncontracted Slater-type orbitals (STOs) with TZ2P quality as basis functions.[30] An auxiliary set of s, p, d,

and f STOs was used to fit the molecular densities and to represent the Coulomb and exchange potentials accurately in each SCF cycle.[31] Scalar relativistic effects have been taken into account by ZORA. Further details on the EDA can be found in SI and literature.[15]

Throughout our papers we use as an indicator of stability the bond dissociation energy, D_e, where:

$$-D_e = \Delta E \text{ for the reaction fragments} \leftrightarrow \text{molecule.}$$

For instance, $-D_e = E(\text{adduct}) - E(\text{metal fragment}) - E(SO_2)$, each optimized separately. D_e is a positive quantity, when the adduct is more stable than the fragments.

ASSOCIATED CONTENT

Supporting Information

Computational details; Coordinates and energies of all calculated model adducts; NBO charges and Wiberg bond orders for all atoms in the calculated complexes.

AUTHOR INFORMATION

Corresponding Author

andrey.rogachev@iit.edu

Notes

The authors declare no competing financial interest

ACKNOWLEDGEMENTS

REFERENCES

[1] (a) Lewis, G.N. *J. Am. Chem. Soc.*, **1916**, *38*, 762. (b) Lewis, G.N. *Valence and the Structure of Atoms and Molecules*, Chemical Catalog Co, 1st Ed., **1923**, p. 172. (c) Crabtree, R.H. *The Organometallic Chemistry of the Transition Metals*, WILEY *Inc.*, **2009**. (d) Hartwig, J. *Organotransition Metal Chemistry*, University Science Books, **2010**. (e) *Comprehensive Coordination Chemistry* II, Eds. McCleverty, J.A.; Meyer, T.J. Elsevier Science, **2005**, p. 9500.

[2] Pauling, L. "*Nature of the Chemical Bond*", Cornel University Press, 2nd Ed., Ithaca, NY, USA. **1947**, 251.

[3] (a) Enemark, J.H.; Feltham, R.D. *Coord. Chem. Rev.* 1974, *13*,339. (b) Jørgenson, C.K. *Coord. Chem. Rev.* **1962**, *1*, 164; Schonherr, T. *Struct Bond.* **2004** *106*, 1. (c) Nugent, W.A.; Mayer, J.M. "*Metal-Ligand Mutiple Bonds*", Wiley Interscience, New York, USA. **1988**.

[4] (a) Amgoune, A.; Bourissou, D. *J. Chem. Soc., Chem. Commun.*, **2011**, *47*, 859. (b) Parkin, G. *Organometallics*, **2006**, *25*, 4744.

[5] (a) Crossley, I.R.A.; Hill, A.F.; Willis, A.C. *Organometallics*, **2006**, *25*, 289. (b) Hill, A. *Organometallics*, **2006**, *25*, 4741.

[6] (a) Braunschweig, H.; Grass, K.; Radacki, K. *Angew. Chem., Int. Ed.*, **2005**, *46*, 7782. (b) Braunschweig, H., Dewhurst, R.D., Schneider, A. *Chem. Rev.*, **2010**, *110*, 3924. (c) Bauer, J., Braunschweig, H., Dewhurst, R.D. *Chem. Rev.*, **2012**, *112*, 4329.

[7] Rogachev, A.Yu.; Hoffmann, R. *J. Am. Soc. Chem.*, **2013**, *135*, 3262.

[8] Glue, V.K.; Brunel, W.; Rehm, K. *Z. Anorg. Allg. Chem.* **1938**, *235*, 201.

[9] (a) Ryan, R.R.; Eller, R.G. *Inorg. Chem*, **1976**, *15*, 494. (b) Mingos. D.P. *Transition Met. Chem.*, **1978**, *3*, 1. (c) Ryan, R.R.; Kubas, G.J.; Moody, D.C.; Eller, P. G. *Struct. Bond.*, **1981**, *46*, 47.

[10] Mingos, D.M.P. *Struct. Bond.*, **2014**, *154*, 1.

[11] (a) Terheijden, J.; van Koten, G.; Mul, W.P.; Stufkens, D.J. *Organometallics*, **1986**, *5*, 519. (b) Albrecht, M.; Gossage, R.A.; Lutz, M.; Spek, A.L.; van Koten, G. *Chem. Eur. J.*, **2000**, *6*, 1431. (c) Steenwinkel, P.; Kooijman, H.; Smeets, W.J.J.; Spek, A.L.; Grove, D.M.; van Koten. G. *Organometallics*, **1998**, *17*, 5411. (d) Albrecht, M.; Gossage, R.A.; Frey, U.; Ehlers, A.W.; Baerends, E.J.; Merbach, A.E.; van Koten, G. *Inorg. Chem.*, **2001**, *40*, 850. (e) Albrecht, M.; Luts, M.; Schreurs, A.M.M.; Lutz, E.T.H.; Spek, A.L.; van Koten, G. *J. Chem. Soc., Dalton Trans.*, **2000**, 3797. (f) Albrecht, M.; Lutz, M.; Spek, A.L.; van Koten, G. *Nature*, **2000**, *406*, 970.

[12] (a) Mingos, D.M.P. *J. Organomet. Chem.*, **2014**, *751*, 153-173. (b) Schenk, W.A. *Dalton Trans.*, **2011**, *40*, 1209. (c) Schenk, W.A. *Angew. Chem., Int. Ed.*, **1987**, *26*, 98.

[13] (a) Retzer, H.J.; Gilbert, T.M. *Inorg. Chem.* **2003**, *42*, 7207. (b) Brust D.J.; Gilbert, T.M. *Inorg. Chem.* **2004**, *43*, 1116.

[14] (a) Weinhold, F.; Landis, C. A. *Valency and Bonding: A Natural Bond Orbital Donor – Acceptor Perspective*, Cambridge University Press: Cambridge, **2005**. (b) Reed, A. E.; Curtiss, L.A.; Weinhold, F. *Chem. Rev.*, **1988**, *88*, 899.

[15] (a) Lein, M.; Frenking, G. in *Theory and Application of Computational Chemistry*, ed. Dekstra, C. **2005**. (b) von Hopffgarten, M.; Frenking, G. in *Computational Inorganic and Bioinorganic Chemistry*, ed. E. Solomon, **2009**, pp. 3-15. (c) Lein, M.; Szabo, A.; Kovac, A.; Frenking, G. *Faraday Discuss.*, **2003**, *124*, 365. (d) Frenking, G.; Wichmann, K.; Frohlich, N.; Loschen, C.; Lein, M.; Frunzke, J.; Rayon, V. M. *Coord. Chem. Rev.*, **2003**, *238-239*, 55-82. (e) Krapp, A.; Bickelhaupt, F. M.; Frenking, G. *Chem. Eur. J.*, **2006**, *12*, 9196-9216. (f) Krapp, A.; Frenking, G. *J. Comput. Chem.*, **2007**, *28*, 15-24. (g) von Hopffgarten, M.; Frenking, G. *WIREs Comput. Mol. Sci.*, **2012**, *2*, 9196.

[16] (a) Arifhodzic-Radojevic, S.; Burrows, A.D.; Choi, N.; McPartlin, M.; Mingos, D.M.P.; Tarlton, S.V.; Vilar, R. *J. Chem. Soc., Dalton Trans.*, **1999**, 3981. (b) Ritchey, J.M.; Moody, D.C.; Ryan, R.R. *Inorg. Chem.*, **1983**, *22*, 2276. (c) Moody, D.C.; Ryan, R.R. *Inorg. Chem.*, **1976**, *15*, 1823.

[17] (a) Ibrahim Al-Rafia, S.M.; Malcolm, A.C.; Liew, S.K.; Ferguson, M.J.; Rivard, E. *J. Am. Chem. Soc.*, **2011**, *133*, 777. (b) Dostálová, R.; Dostál, L.; Růžička, A.; Jambor, R. *Organometallics*, **2011**, *30*, 2405. (c) Ibrahim Al-Rafia, S.M.; Malcolm, A.C.; McDonals, R.; Ferguson, M.J.; Rivard, E. *Angew. Chem. Int. Ed.*, **2011**, *50*, 8354. (d) Spinney, H.A.; Piro, N.A.; Cummins, C.C. *J. Am. Chem. Soc.*, **2009**, *131*, 16233. (e) Cossairt, B.M.; Piro, N.A.; Cummins, C.C. *Chem. Rev.*, **2010**, *110*, 4164. (f) Piro, N.A.; Cummins, C.C. *J. Am. Chem. Soc.*, **2008**, *130*, 9524. (g) Piro, N.A.; Cummins, C.C. *Angew. Chem. Int. Ed.*, **2009**, *48*, 934. (h) Piro, N.A.; Cummins, C.C. *Inorg. Chem.*, **2007**, *46*, 7387.

[18] Rogachev, A.Yu.; Hoffmann, R. *Inorg. Chem.*, **2013**, *52*, 7161.

[19] (a) Hillier, I.H.; Saunders, V.R. *Chem. Phys. Lett.*, **1969**, *4*, 163. (b) Dacre, P.D.; Elder, M. *Theor. Chim. Acta*, **1972**, *25*, 254. (c) Roos, B.; Siegbahn, P. *Theor. Chim. Acta*, **1971**, *21*, 368.

[20] (a) Rogachev, A.Yu.; Petrukhina, M.A. *J. Phys. Chem. A*, **2009**, *113*, 5743. (b) Filatov, A.S.; Rogachev, A.Yu.; Jackson, E.A.; Scott, L.T.; Petrukhina, M.A. *Organometallics*, **2010**, *29*, 1231. (c) Filatov, A.S.; Rogachev, A.Yu.; Petrukhina, M.A. *Cryst. Growth Des.*, **2006**, *6*, 1479. (d) Cotton, F.A.; Dikarev, E.V.; Petrukhina, M.A. *Angew. Chem., Int. Ed.*, **2000**, *39*, 2362. (e) Cotton, F.A.; Dikarev, E.V.; Petrukhina, M.A. *Angew. Chem., Int. Ed.*, **2001**, *40*, 1521.

[21] *See for instance*: (a) Oh, J.J.; LaBarge, M.S.; Matos, J.; Kampf, J.W.; Hilling II, K.W.; Kuczkowski, R.L. *J. Am. Chem. Soc.*, **1991**, *113*, 4732. (b) Denk, M.K.; Hatano, K.; Lough, A.J. *Eur. J. Inorg. Chem.*, **2003**, 224.

[22] (a) Perdew, J.P.; Burke, K.; Ernzerhof, M. *Phys. Rev. Lett.*, **1997**, *78*, 1396. (b) Perdew, J.P.; Burke, K.; Ernzerhof, M. *Phys. Rev. Lett.*, **1996**, *77*, 3865.

[23] (a) Pantazis, D.A.; Chen, X.-Y.; Landis, C.R.; Neese, F. *J. Chem. Theory Comput.*, **2008**, *4*, 908. (b) Buhl, M.; Reimann, C.; Pantazis, D.A.; Bredow, T.; Neese, F. *J. Chem. Theory Comput.*, **2008**, *4*, 1449, (c) DeBeer George, S.; Neese, F. *Inorg. Chem.*, **2010**, *49*, 1849.

[24] Neese, F.; Wennmohs, F.; Hansen, A.; Becker, U. *Chem. Phys.*, **2009**, *356*, 98.

[25] Neese, F. *Wiley Interdiscip. Rev.: Comp. Mol. Sci.*, **2012**, 2, 73.

[26] Wiberg, K. B. *Tetrahedron* **1968**, *24*, 1083.

[27] (a) Glendening, E.D.; Badenhoop, J.K.; Reed, A. E.; Carpenter, J.E.; Bohmann, J.A.; Morales, C.M.; Weinhold, F. *NBO 6.0*, **2013**, University of Wisconsin, Madison. (b) Glendening, E.D.; Landis, C.R.; Weinhold, F. *J. Comp. Chem.*, **2013**, *34*, 1429.

[28] (a) Morokuma, K. *J. Chem. Phys.*, **1971**, *55*, 1236. (b) Ziegler, T.; Rauk, A. *Inorg. Chem.*, **1979**, *18*, 1558. (c) Ziegler, T.; Rauk, A. *Inorg. Chem.*, **1979**, *18*, 1755.

[29] (a) Fonseca Guerra, C.; Snijders, J. G.; te Velde, G.; Baerends, E. J. *Theor. Chem. Acc.*, **1998**, *99*, 391. (b) *ADF2008.01*, SCM, Vrije Universiteit, Amsterdam, Netherlands, http://www.scm.com. (c) te Velde, G.; Bickelhaupt, F. M.; Baerends, E. J.; Fonseca Guerra, C.; van Gisbergen, S. J. A.; Snijders, J. G.; Ziegler, T. *J. Comput. Chem.*, **2001**, *22*, 931.

[30] Snijders, J. G.; Baerends, E. J.; Vernooijs, P. *At. Data Nucl. Data Tables*,, **1982**, *26*, 483.

[31] Krijn, J.; Baerends, E. J. *Fit Functions in the HFS-Method*, **1984**, Internal Report (In Dutch), Vrije Universiteit, Amsterdam, Netherlands.

For Table of Contents Only

LP(S) → σ*(Rh - Rh)

vs.

d$_{z^2}$(Pt) → LAO(S)
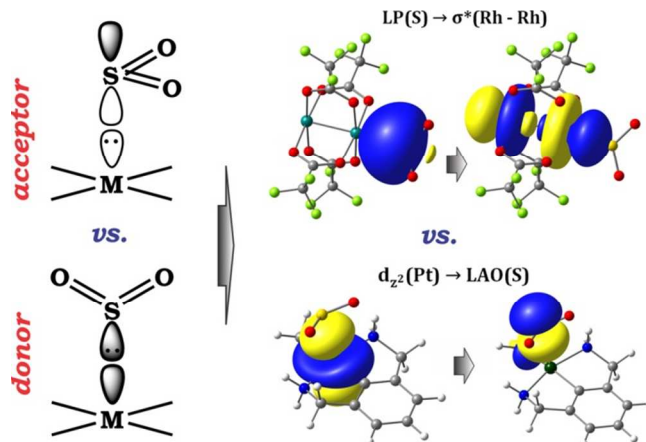
The SO$_2$ molecule represents the unique class of systems, which show two-faced behavior. This is the case when the molecule can act as a donor or an electron acceptor through the same atom, depending on the environment. In this article, we report the first comprehensive theoretical investigation of the behavior of SO$_2$ molecule in reaction with different (Lewis acidic or basic) organometallic fragments. Orbital interactions in such adducts were analyzed in detail.